# Cage correlation and diffusion in strongly coupled three-dimensional Yukawa systems in magnetic fields

K. N. Dzhumagulova,[1] R. U. Masheyeva,[1] T. Ott,[2] P. Hartmann,[3] T. S. Ramazanov,[1] M. Bonitz,[2] and Z. Donkó[3]

[1]*IETP, Al Farabi Kazakh National University, 71, al Farabi Avenue, Almaty, 050040, Kazakhstan*

[2]*Institute for Theoretical Physics and Astrophysics, Christian-Albrechts-University Kiel, Leibnizstrasse 15, 24098 Kiel, Germany*

[3]*Institute for Solid State Physics and Optics, Wigner Research Centre for Physics, Hungarian Academy of Sciences, H-1121 Budapest, Konkoly-Thege Miklós Street 29-33, Hungary*

The influence of an external homogeneous magnetic field on the quasilocalization of the particles—characterized quantitatively by cage correlation functions—in strongly coupled three-dimensional Yukawa systems is investigated via molecular dynamics computer simulations over a wide domain of the system parameters (coupling and screening strengths, and magnetic field). The caging time is found to be enhanced by the magnetic field **B**. The anisotropic migration of the particles in the presence of magnetic field is quantified via computing directional correlation functions, which indicate a more significant increase of localization in the direction perpendicular to **B**, while a moderate increase is also found along the **B** field lines. Associating the particles' escapes from the cages with jumps of a characteristic length, a connection is found with the diffusion process: the diffusion coefficients derived from the decay time of the directional correlation functions in both the directions perpendicular to and parallel with **B** are in very good agreement with respective diffusion coefficients values obtained from their usual computation based on the mean-squared displacement of the particles.

## I. INTRODUCTION

Strongly coupled plasmas are characterized by a pair-interaction potential energy that dominates over the kinetic energy of the particles. Systems with this property are rather widespread in nature and appear as well in various laboratory settings [1]. A wide variety of physical phenomena taking place in such a system makes them an attractive subject for investigations [2–4]. Strongly coupled plasmas are used in many areas of science and technology that are continuously expanding, and studies are performed by both experimental [5,6] and theoretical methods [7–9].

One of the prominent features of strongly coupled plasmas is the quasilocalization of particles: the particles spend substantial time in local minima of the slowly varying potential surface developing in such systems. However, the localization time is limited by the changing of the potential surface due to the diffusion of the particles. It is noted that this behavior of the particles is an important underlying assumption of the quasilocalized charge approximation (QLCA) developed by Golden and Kalman [10], which is an important theoretical method in many-body physics, allowing the derivation of wave dispersion relations in strongly coupled plasmas from static properties (pair correlation function) of the systems.

The localization of individual particles and the changes in their surroundings can be quantified by adopting a correlation method, which was introduced in Refs. [11,12]. This method has already been applied in molecular dynamics simulation studies of the localization time of particles in strongly coupled Coulomb and Yukawa systems [13,14]. These investigations have confirmed that in the strongly coupled liquid phase, the localization (or "caging") time covers several plasma oscillation periods in these settings.

Recently, much attention was paid to the physics of dusty plasmas under the effect of external magnetic fields [15–25]. The influence of a magnetic field on the dynamics of one-component [15,16] and binary Yukawa systems [16] have been analyzed. In these works, molecular dynamics simulations have been used for the calculation of the diffusion coefficient of the particles on the basis of the mean-square displacement. The influence of an external magnetic field on the velocity autocorrelation function of the particles and the cage correlation functions in two-dimensional strongly coupled Yukawa systems was investigated in Ref. [17]. In Refs. [26,27], an approach to achieve very strong magnetization has been proposed, which is based on the equivalence of the magnetic Lorentz force and the Coriolis inertial force acting on moving objects in a rotating reference frame. Experimental realization of a rotating dusty plasma has shown the formation of magnetoplasmons [27] in the quasimagnetized dusty plasma. Also, the generation of higher harmonics of the magnetoplasmon frequency in strongly coupled two-dimensional plasma liquids has been reported in Refs. [18,19].

The purpose of this work is to investigate the influence of a homogeneous magnetic field on the particles' localization that is quantified by *cage correlation functions*. As the external magnetic field breaks the symmetry of the system, directional cage correlation functions are also calculated along the magnetic field direction and perpendicular to it. A connection is established between the random events of single particle escapes from the cages and the self-diffusion coefficient of the particles obtained from the mean-square displacement of the particles. Section II describes the model system and the computational procedures. The results are presented in Sec. III, while a brief summary is given in Sec. IV.

## II. MODEL AND SIMULATION METHOD

For our model system we adopt the screened Coulomb (Debye-Hückel or Yukawa) potential of the form

$$\phi(r) = \frac{Q}{4\pi\varepsilon_0} \frac{\exp(-r/\lambda_{\mathrm{D}})}{r}, \tag{1}$$

where $Q$ is the charge of the particles and $\lambda_D$ is the screening (Debye) length. The ratio of the potential energy to the thermal energy is expressed by the coupling parameter

$$\Gamma = \frac{Q^2}{4\pi\varepsilon_0 a k_B T}, \tag{2}$$

where $T$ is the temperature, $a = [3/(4\pi n)]^{1/3}$ is the three-dimensional Wigner-Seitz radius, and $n$ is the particle number density.

A homogeneous external magnetic field with an induction vector $\mathbf{B} = (0,0,B)$ is imposed on the system and the strength of this field is characterized by the dimensionless parameter

$$\beta = \frac{\omega_c}{\omega_p}, \tag{3}$$

where $\omega_c = QB/m$ is the cyclotron frequency and $\omega_p = \sqrt{nQ^2/\varepsilon_0 m}$ is the plasma frequency. The parameter $\beta$, together with the two other dimensionless quantities $\Gamma$ and $\kappa = a/\lambda_D$ (the screening parameter), characterize the system completely.

To investigate the localization of particles the changes of the surroundings of individual particles are monitored through the correlation technique developed in Refs. [11,12]. Following this formalism, a neighbor list $\ell_i$ is defined for particle $i$ as

$$\ell_i = \{f_{i,1}, f_{i,2}, \dots, f_{i,N}\}, \tag{4}$$

where $f_{ij} = \Theta(r_c - r_{ij})$ with $r_{ij} = |\vec{r}_i - \vec{r}_j|$ and $\Theta$ is the Heaviside function (i.e., $f_{ij} = 1$ if $r_{ij} \leqslant r_c$, and $f_{ij} = 0$ otherwise). Here, $r_c$ is the cage radius, and the condition $r_{ij} \leqslant r_c$ reflects that the neighbors are closely separated (elements with $i = j$ are omitted from the neighbor list).

The cage radius is chosen here as $r_c = 2.42$, which well approximates the position of the first minimum of the pair correlation function, $g(r)$, at high coupling values. (We note that the same value has been used in previous studies of caging in one-component plasmas [14,15].) This choice expresses that the neighbor particles belong to the first coordination shell. Our computations of the coordination number $\int_0^{r_c} rg(r)dr$ resulted in values near 14, which is the sum of the closest and second closest neighbors both in bcc and fcc lattices. In the liquid phase, these particles form an unresolvable common shell around the test particles. (Note that in the strongly coupled liquid phase the pair correlation function reflects the underlying lattice configuration, which is bcc for $\kappa = 1$ and bcc or fcc for $\kappa = 2$ [28].)

The number of particles that have left the original cage of particle $i$ at time $t$ can be determined as

$$n_i^{\text{out}}(t) = |\ell_i(0)^2| - \ell_i(0) \cdot \ell_i(t). \tag{5}$$

The first part of this equation defines the number of particles around particle at time $t = 0$, while the second term defines the number of particles that remained in the surrounding after time $t$.

The cage correlation function (CCF), which expresses the probability of the escape of less than $c$ particles from the cage, can be calculated by averaging over particles and initial times, the function $\Theta(c - n_i^{\text{out}})$:

$$C^{(c)}(t) = \left\langle \Theta\left(c - n_i^{\text{out}}(0,t)\right) \right\rangle. \tag{6}$$

The CCF can be obtained for different values of $c$. The cages are defined here to be decorrelated when the $C^{(c)}(t)$ function decays to 0.1, with $c = 7$, i.e., the number of particles that leave the cage is set to half of the number of particles within the first coordination shell (in the liquid phase).

In our system, where the external magnetic field breaks the isotropy, it is sensible to investigate the departure of the neighbors of test particles into *different directions*. This can be performed via the "directional correlation functions" (DCF) $F_x^{(c)}(t)$, $F_y^{(c)}(t)$, and $F_z^{(c)}(t)$, which [taking $F_x^{(c)}(t)$ as an example] can be defined as

$$f_{ij,x}(t) = \begin{cases} 1 & \text{if } x_{ij} < r_c, \\ 0 & \text{if } x_{ij} \geqslant r_c, \end{cases} \tag{7}$$

$$n_{i,x}^{\text{out}}(t) = |\ell_{i,x}(0)^2| - \ell_{i,x}(0) \cdot \ell_{i,x}(t), \tag{8}$$

$$F_x^{(c)}(t) = \left\langle \Theta\left(c - n_{i,x}^{\text{out}}(0,t)\right) \right\rangle, \tag{9}$$

where $x_{ij} = |x_i - x_j|$ is the distance in $x$ direction between the $i$th and $j$th particles. [For $F_y^{(c)}(t)$ and $F_z^{(c)}(t)$ we use equivalent definitions.] It is important to note that while the above definitions strongly resemble the definitions of the cage correlation function, the directional correlation function for a *given* direction may still keep its high value even after a significant displacement of the particles in *another* direction took place. So, a high value of these functions does not necessarily indicate a caged state. For the computations of the escape functions we use $N = 1000$ particles in the MD simulations.

In order to calculate the diffusion coefficient from the equilibrium dynamics, we employ the Einstein relation for the mean-squared displacement [29], i.e.,

$$D_\mu = \lim_{t\to\infty} \frac{\langle|\mu(t) - \mu(t_0)|^2\rangle}{2t}, \tag{10}$$

where $\mu = x,y,z$ and $\langle\dots\rangle$ denotes averaging over the entire particle ensemble. Note that Eq. (10) is only valid for normal diffusion, i.e., when the mean-squared displacement grows linearly with time. In a two-dimensional system, this is not always the case, see, e.g., Refs. [16,30,31] for observations of "superdiffusion." Such deviation from normal diffusion was not observed in our 3D system.

Equation (10) is evaluated for $N = 8192$ particles at $\omega_p t = 5000$ [32]. As the magnetic field is aligned along the $z$ axis, we expect that (i) the self-diffusion coefficients measured in the field-perpendicular directions are the same, i.e., $D_x = D_y = D_\perp$, and (ii) a different self-diffusion coefficient, $D_z = D_\parallel$, is found in the field-parallel direction [16].

## III. RESULTS

In the following (in Sec. III A) we present representative results obtained for the overall (directionally not resolved) cage correlation functions for a wide domain of the system parameters $\Gamma$, $\kappa$, and $\beta$. Next, in Sec. III B, we consider the directional cage correlation functions and examine their behavior, while in Sec. III C, we discuss the connection between the cage correlation functions and the self-diffusion coefficient of the system.
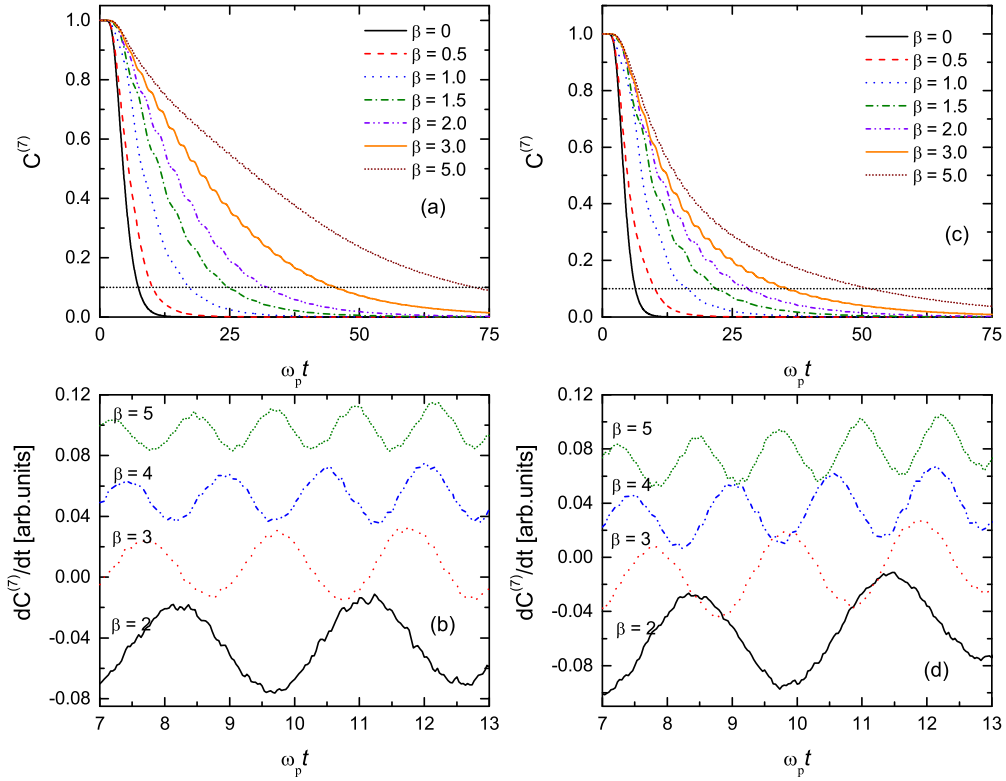
FIG. 1. Cage correlation functions $C^{(7)}(t)$ (a, c) and their derivative with respect to time (b, d) obtained for different values of $\beta$ at $\Gamma = 10$, $\kappa = 1$ (a, b)and $\kappa = 2$ (c, d). Panels (a) and (c) also indicate a line $C^{(7)} = 0.1$ that defines the caging time. In panels (b) and (d), the different curves are shifted vertically for clarity.
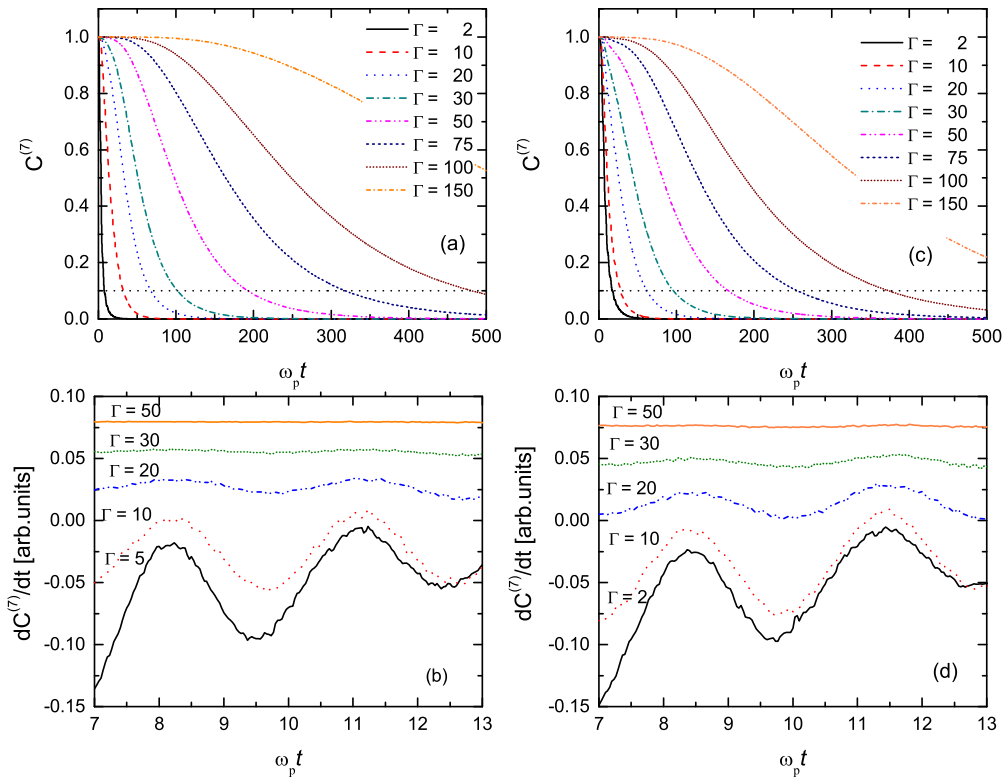


FIG. 2. Cage correlation functions $C^{(7)}(t)$ (a, c) and their derivative with respect to time (b, d), obtained for different values of $\Gamma$ at $\beta = 2$, $\kappa = 1$ (a, b) and $\kappa = 2$ (c, d). Panels (a) and (c) also indicate a line $C^{(7)} = 0.1$ that defines the caging time. In panels (b, d), the different curves are shifted vertically for clarity.

## A. Cage correlations

Figures [1(a)] and [1(c)] present cage correlation functions obtained at $\Gamma = 10$ and, respectively, for $\kappa = 1$ and $\kappa = 2$, for a series of magnetic field strengths $0 \leqslant \beta \leqslant 5$. Recall that the caging time $t_{cage}$ is defined through $C^{(7)} = 0.1$. For $\kappa = 1$, the caging time at zero magnetic field is found to be $\omega_p t_{cage} \approx 8$, which corresponds to approximately one plasma oscillation cycle. This "weakly caged" behavior changes significantly when a magnetic field is applied: At $\beta = 3$, the caging time increases by about a factor of six. A similar dependence is obtained at $\kappa = 2$ [see Fig. [1(c)]].

The curves depicted in Figs. [1(a)] and [1(c)], especially the ones that correspond to intermediate values of $\beta$, exhibit "ripples," which can be emphasized by taking the time derivatives of these curves. These derivatives are shown in Figs. [1(b)] and [1(d)], for selected $\beta$ values. The dominant frequency in these curves turns out to be proportional to the magnetic field strength and, based on this observation, the occurrence of these oscillations can be explained by the effect that particles leave and reenter the cages, while moving on cyclotron orbits. Indeed, measurements of the frequencies $\omega^*$ of the $dC^{(7)}/dt$ curves confirms $\omega^* \cong \omega_c$. The amplitude of oscillations of $dC^{(7)}/dt$ decay in amplitude with increasing $\beta$ because of the decreasing Larmor radius of the particle trajectories that results in a diminishing importance of the leaving-reentering effect. At low $\beta$ values, on the other hand, the oscillations are less visible too, as caging itself is less pronounced and the cage correlation curve already decays on the timescale of the inverse cyclotron frequency.

The dependence of the cage correlation function on the coupling parameter $\Gamma$ is revealed in Figs. [2(a)] and [2(c)], at $\kappa = 1$ and $\kappa = 2$, respectively, for a fixed magnetic field of $\beta = 2$. The increasing coupling results in a significant enhancement of the caging time. At high coupling the cage correlation function decays to 0.1 at $\omega_p t$ values of several hundreds, meaning the particles undergo several tens to hundreds of plasma oscillations within their cages. These numbers are conceivable, as the highest $\Gamma$ values correspond to about 70% and 45% of the critical values for the fluid-solid phase transition (which are $\Gamma = 217$ and 440, respectively, for $\kappa = 1$ and 2 [33]), and the caging time in the solid phase is trivially infinite.

Examination of the dependence of $dC^{(7)}/dt$ on the coupling strength [see Figs. [2(b)] and [2(d)]] reveals that the oscillations diminish with increasing $\Gamma$ and disappear at a value of $\Gamma \approx 50$. The decreasing amplitude of the oscillations can be attributed to the fact that at higher coupling the cages are more rigid and the reduced thermal energy of the particles results in smaller Larmor radii.

The results obtained for the caging time of the particles are shown in Fig. [3]. Figure [3(a)] displays the dependence of $t_{cage}$ on the magnetic field strength at selected $\Gamma$ values, while Fig. [3(b)] shows the dependence on $\Gamma$ at fixed $\beta$ values. In the first case we find a nearly linear increase of the caging time with $\beta$, while the connection between $t_{cage}$ and $\Gamma$ is nearly a power-law function. Apart from few data points at low $\Gamma$, the curves in Fig. [3(b)] that belong to different $\beta$ values are nearly parallel, indicating a universal behavior.
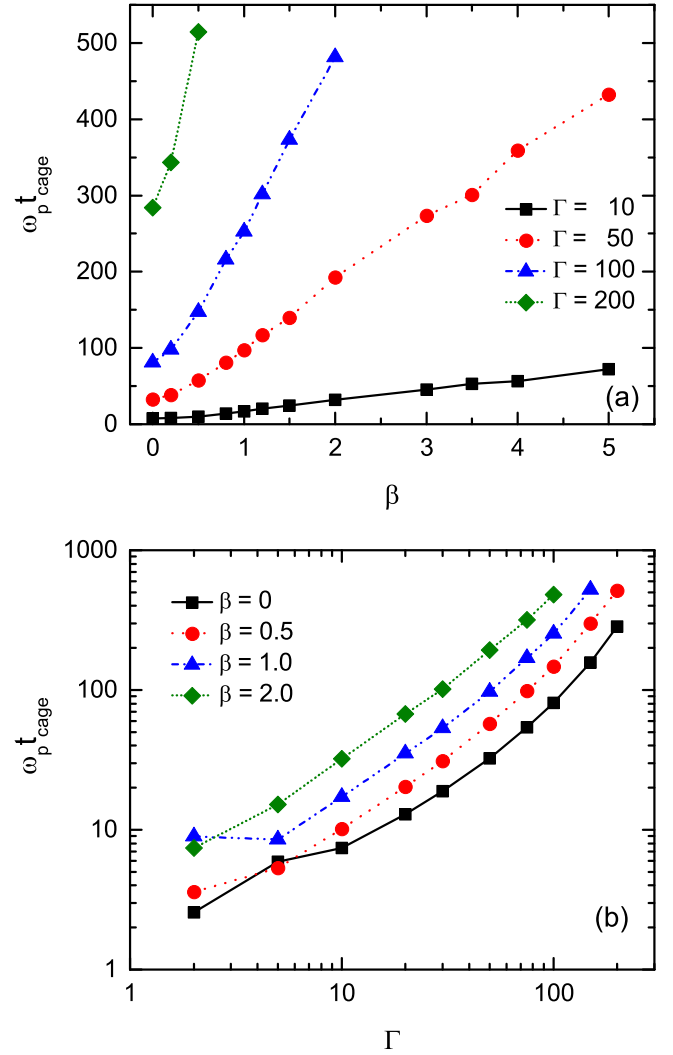


FIG. 3. Dependence of caging time on the strength of magnetic field $\beta$ (a) and on the coupling parameter $\Gamma$ (b), at $\kappa = 1$.

## B. Directional correlation functions

The anisotropy of the system established at $\mathbf{B} \neq 0$ suggests that different escape rates from the cages in the field-perpendicular and field-parallel directions may exist. To demonstrate this behavior we have computed the directional correlation functions introduced in Sec. [II] [see Eqs. [(7)]–[(9)]]. The results of these calculations are shown in Fig. [4] for $\Gamma = 10$ and $\kappa = 1$. Figure [4(a)] corresponds to the very low magnetic field of $\beta = 0.001$, where we find equal correlation functions in all directions, $F_x^{(7)}(t) = F_y^{(7)}(t) = F_z^{(7)}(t)$, within the limits of errors. When the magnetic field is increased [see Fig. [4(b)] for $\beta = 0.5$], a significantly stronger confinement (slower decay of the directional correlation function) is found in the $x$ and $y$ directions, i.e., perpendicularly to the direction of the magnetic field, as compared to the field-parallel direction. The effect further amplifies when $\beta$ reaches higher values, as shown in Fig. [4(c)] for the strong magnetic field case with $\beta = 2$. While the blocking of diffusion along the field-perpendicular direction is almost a trivial result, the increase of the decay
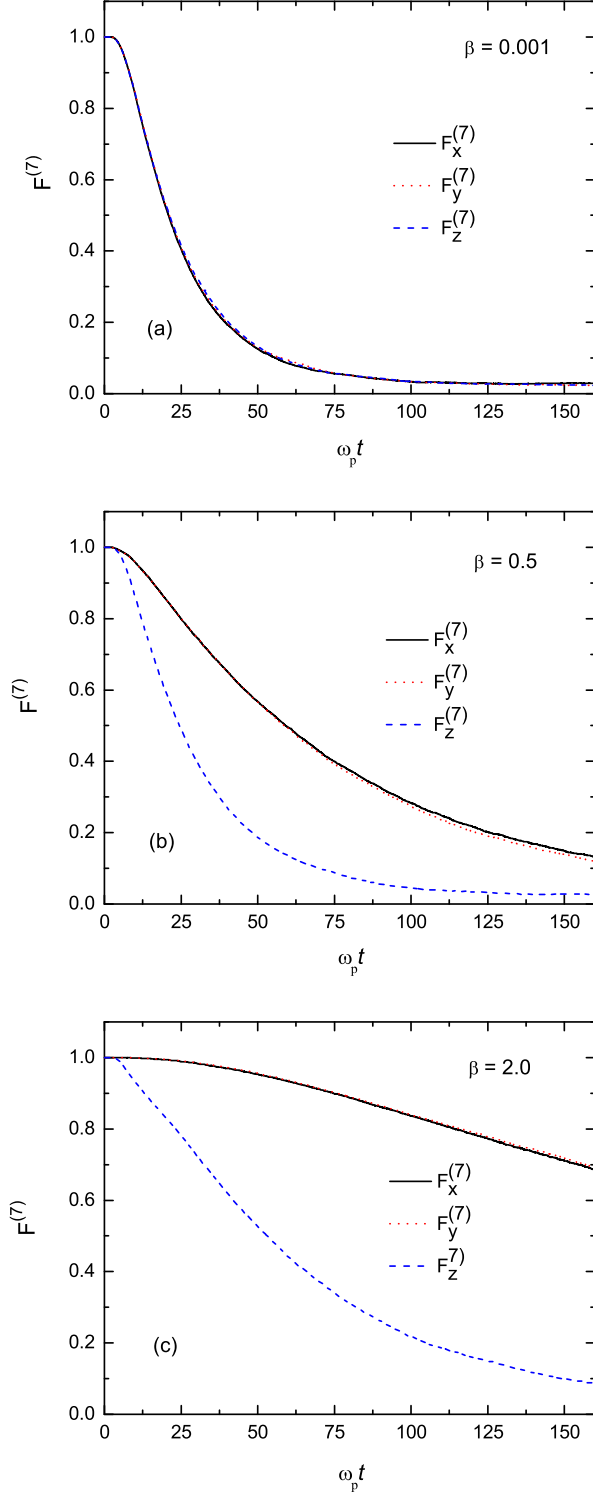
FIG. 4. Directional correlation functions obtained for different values of the magnetic field strength: (a) $\beta = 0.001$, (b) $\beta = 0.5$, and (c) $\beta = 2$, at $\Gamma = 10$ and $\kappa = 1$.

time along the field-parallel direction with increasing $\beta$ is less expected, but this effect is also clearly observed via the quantification of the directional correlations functions; compare the $F_z^{(7)}(t)$ curves in the panels of Fig. 4.

### C. Connection between the directional correlation functions and the self-diffusion

A link between the escapes (or "jumps") of single particles out of the particles' surroundings and the process of self-diffusion can be established as follows. As explained above, the cage correlation function $C^{(c)}(t)$ gives the probability of the escape of less than $c$ particles from the cage. Similarly, $F^{(c)}(t)$ gives the probability of the escape of less than $c$ particles from the vicinity of a test particle, *in a given direction*. The probability of the escape of *exactly one* particle can thus be calculated as

$$P_1(t) = F^{(2)}(t) - F^{(1)}(t). \tag{11}$$

We find that $P_1$ exhibits an exponential decay (except at early times),

$$P_1(t) = A \exp(-t/t_0), \tag{12}$$

where the characteristic time $t_0$, related to jumps of single particles, is a function of the system parameters ($\Gamma$, $\kappa$, and $\beta$). We assign a characteristic length $\delta$ to these jumps, which makes it possible to calculate a diffusion coefficient [14]:

$$D_c = \frac{\delta^2}{t_0}. \tag{13}$$

By adopting a fixed value for $\delta$, the diffusion coefficient computed in this manner can be compared with diffusion coefficients computed from MD simulations via the mean-squared displacement (MSD). Figure 5 shows the comparison between the diffusion coefficients $D^* = D/(\omega_p a^2)$ based on MSD and those obtained from the present directional correlation functions, adopting a value of $\delta/a = 0.71$ for the characteristic length of jumps. This value of $\delta$, which results in the best agreement between the diffusion coefficient values obtained in the two independent ways is close to the mean particle separation $\sim a$, so it can be considered as a reasonable value for jump events when two particles switch positions. The self-diffusion coefficients obtained via the two independent ways show a remarkable agreement for all the coupling, screening, and magnetic field strength values considered. At $\beta = 0$, as shown in Fig. 5(a), the diffusion coefficient is "isotropic," i.e., is equal in all directions. With the growth of the magnetic field the difference between the diffusion coefficients in the field-perpendicular and the field-parallel directions increases; see Figs. 5(b)–5(d).

## IV. CONCLUSIONS

We have investigated the effect of a homogeneous magnetic field on the cage correlation functions in three-dimensional strongly coupled Yukawa liquids, for a wide range of system parameters: the coupling parameter, the strength of magnetic field, and the screening parameter. The results show that both with an increasing magnetic field strength ($\beta$) and an increasing coupling strength ($\Gamma$), the caging time is significantly prolonged due to the decreasing Larmor radius of the particle trajectories and the reduced thermal fluctuations. Oscillations of the cage correlation functions at $\beta > 0$ arise from the gyrating motion of particles close to the cage boundaries.

The directionally resolved correlation functions were found to reflect the anisotropy of the system created by the magnetic field **B**. The decay time of these functions increased
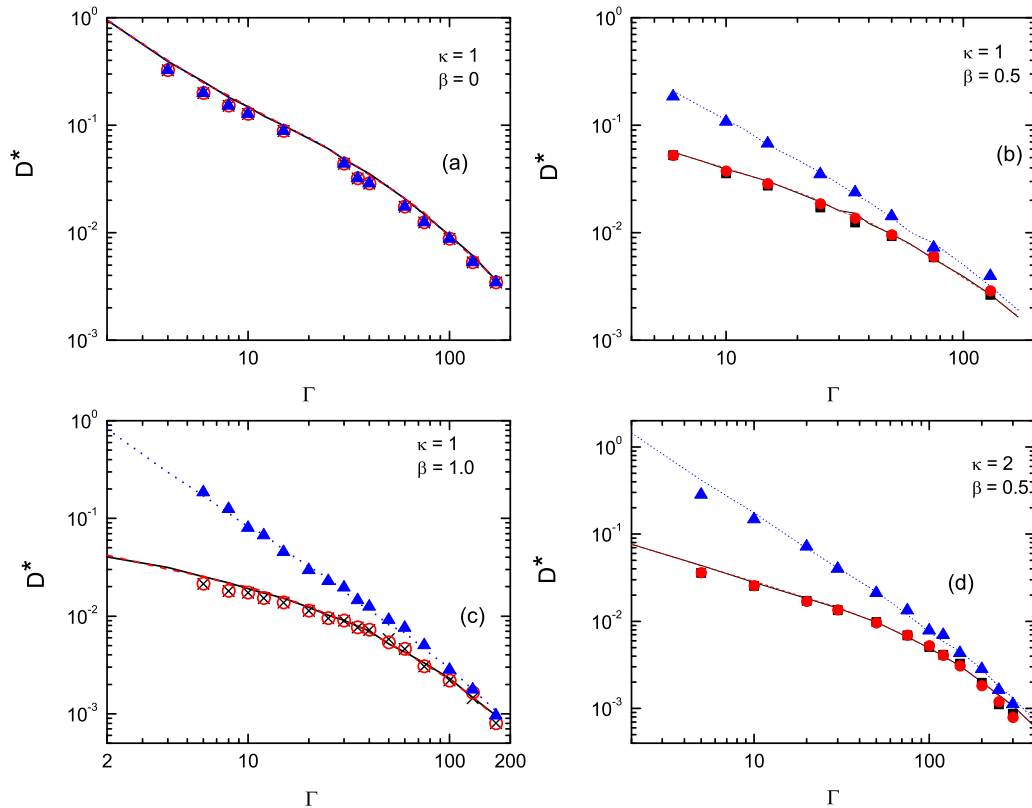
FIG. 5. Normalized "directional" diffusion coefficients, $D^* = D/\omega_p a^2$, as obtained from mean-squared displacements of the particles (lines) and from the directional correlation functions (symbols). (a) $\kappa = 1$, $\beta = 0$, (b) $\kappa = 1$, $\beta = 0.5$, (c) $\kappa = 1$, $\beta = 1$, and (d) $\kappa = 2$, $\beta = 0.5$. $\times$ $D_x^*$, $\circ$ $D_y^*$, $\triangle$ $D_z^*$; ——— $D_x^*$, $---$ $D_y^*$, $\cdots$ $D_z^*$.

significantly in the field-perpendicular direction, while a moderate increase was also found in the field-parallel direction.

The self-diffusion coefficient ($D$) of the system was calculated based on the rate of escape of particles into different directions and associating these escape events with jumps of a characteristic length scale. A very good agreement was found across the whole domain of system parameters between $D$ computed this way and via the mean-squared displacement of the particles.

[1] G. J. Kalman, K. Blagoev, and M. Rommel (eds.), *Strongly Coupled Coulomb Systems* (Plenum Press, New York, 1998); V. E. Fortov, A. G. Khrapak, and I. T. Iakubov, *Physics of Strongly Coupled Plasmas* (Oxford University Press, Oxford, 2005).

[2] S. A. Khrapak, M. H. Thoma, M. Chaudhuri, G. E. Morfill, A. V. Zobnin, A. D. Usachev, O. F. Petrov, and V. E. Fortov, Phys. Rev. E **87**, 063109 (2013).

[3] V. E. Fortov and G. E. Morfill, Plasma Phys. Controlled Fusion **54**, 124040 (2012).

[4] O. F. Petrov and V. E. Fortov, Contrib. Plasma Phys. **53**, 767 (2013).

[5] S. A. Maiorov, T. S. Ramazanov, K. N. Dzhumagulova, M. K. Dosbolayev, and A. N. Jumabekov, Phys. Plasmas **15**, 093701 (2008).

[6] G. E. Morfill, H. M. Thomas, U. Konopka, and M. Zuzic, Phys. Plasmas **6**, 1769 (1999).

[7] K. N. Dzhumagulova, T. S. Ramazanov, and R. U. Masheyeva, Contrib. Plasma Phys. **52**, 182 (2012); **53**, 419 (2013); Phys. Plasmas **20**, 113702 (2013).

[8] P. Hartmann, G. J. Kalman, Z. Donkó, and K. Kutasi, Phys. Rev. E **72**, 026409 (2005); G. J. Kalman, P. Hartmann, Z. Donkó, and M. Rosenberg, Phys. Rev. Lett. **92**, 065001 (2004); A. Zs. Kovács, P. Hartmann, and Z. Donkó, Contrib. Plasma Phys. **52**, 199 (2012).

[9] T. Ott, M. Bonitz, Z. Donkó, and P. Hartmann, Phys. Rev. E **78**, 026409 (2008).

[10] G. J. Kalman, K. I. Golden, Z. Donkó, and P. Hartmann, J. Phys. Conf. Series **11**, 254 (2005).

[11] E. Rabani, J. D. Gezelter, and B. J. Berne, J. Chem. Phys. **107**, 6867 (1997).

[12] E. Rabani, J. D. Gezelter, and B. J. Berne, Phys. Rev. Lett. **82**, 3649 (1999).

[13] Z. Donkó, G. J. Kalman, and K. I. Golden, Phys. Rev. Lett. **88**, 225001 (2002).

[14] Z. Donkó, P. Hartmann, and G. J. Kalman, Phys. Plasmas **10**, 1563 (2003).

[15] T. Ott and M. Bonitz, Phys. Rev. Lett. **107**, 135003 (2011).

[16] T. Ott, H. Löwen, and M. Bonitz, Phys. Rev. E **89**, 013105 (2014).

[17] K. N. Dzhumagulova, R. U. Masheeva, T. S. Ramazanov, and Z. Donkó, Phys. Rev. E **89**, 033104 (2014).

[18] M. Bonitz, Z. Donkó, T. Ott, H. Kählert, and P. Hartmann, Phys. Rev. Lett. **105**, 055002 (2010).

[19] T. Ott, M. Bonitz, P. Hartmann, and Z. Donkó, Phys. Rev. E **83**, 046403 (2011).

[20] T. Ott, D. A. Baiko, H. Kählert, and M. Bonitz, Phys. Rev. E **87**, 043102 (2013).

[21] T. Ott, H. H. Kählert, A. Reynolds, and M. Bonitz, Phys. Rev. Lett. **108**, 255002 (2012).

[22] L.-J. Hou, P. K. Shukla, A. Piel, and Z. L. Miskovic, Phys. Plasmas **16**, 073704 (2009).

[23] T. Ott, H. Löwen, and M. Bonitz, Phys. Rev. Lett. **111**, 065001 (2013).

[24] G. Uchida, U. Konopka, and G. Morfill, Phys. Rev. Lett. **93**, 155002 (2004).

[25] K. Jiang, Y.-H. Song, and Y.-N. Wang, Phys. Plasmas **14**, 103708 (2007).

[26] H. Kählert, J. Carstensen, M. Bonitz, H. Löwen, F. Greiner, and A. Piel, Phys. Rev. Lett. **109**, 155003 (2012); M. Bonitz, H. Kählert, T. Ott, and H. Löwen, Plasma Sources Sci. Technol. **22**, 015007 (2013).

[27] P. Hartmann, Z. Donkó, T. Ott, H. Kählert, and M. Bonitz, Phys. Rev. Lett. **111**, 155002 (2013).

[28] S. Hamaguchi, R. T. Farouki, and D. H. E. Dubin, Phys. Rev. E **56**, 4671 (1997).

[29] J. P. Hansen and I. R. McDonald, *Theory of Simple Liquids* (Academic Press, London, 2006).

[30] T. Ott and M. Bonitz, Phys. Rev. Lett. **103**, 195001 (2009).

[31] Yan Feng, J. Goree, Bin Liu, T. P. Intrator, and M. S. Murillo, Phys. Rev. E **90**, 013105 (2014).

[32] Q. Spreiter and M. Walter, J. Comput. Phys. **152**, 102 (1999).

[33] H. Ohta and S. Hamaguchi, Phys. Plasmas **7**, 4506 (2000).